Title
Multiple time scale complexity analysis of resting state FMRI

Journal
Brain Imaging and Behavior, 8(2)

ISSN
1931-7557

Authors
Smith, Robert X
Yan, Lirong
Wang, Danny JJ

Publication Date
2014-06-01

DOI
10.1007/s11682-013-9276-6

Peer reviewed

Brain Imaging and Behavior (2014) 8:284–291
DOI 10.1007/s11682-013-9276-6

SI: GENETIC NEUROIMAGING IN AGING AND AGE-RELATED DISEASES

Multiple time scale complexity analysis of resting state FMRI

Robert X. Smith · Lirong Yan · Danny J. J. Wang

Received: 16 May 2013 / Accepted: 28 October 2013 / Published online: 16 November 2013

Abstract The present study explored multi-scale entropy (MSE) analysis to investigate the entropy of resting state fMRI signals across multiple time scales. MSE analysis was developed to distinguish random noise from complex signals since the entropy of the former decreases with longer time scales while the latter signal maintains its entropy due to a "self-resemblance" across time scales. A long resting state BOLD fMRI (rs-fMRI) scan with 1000 data points was performed on five healthy young volunteers to investigate the spatial and temporal characteristics of entropy across multiple time scales. A shorter rs-fMRI scan with 240 data points was performed on a cohort of subjects consisting of healthy young (age 23 ± 2 years, $n = 8$) and aged volunteers (age 66 ± 3 years, $n = 8$) to investigate the effect of healthy aging on the entropy of rs-fMRI. The results showed that MSE of gray matter, rather than white matter, resembles closely that of f^{-1} noise over multiple time scales. By filtering out high frequency random fluctuations, MSE analysis is able to reveal enhanced contrast in entropy between gray and white matter, as well as between age groups at longer time scales. Our data support the use of MSE analysis as a validation metric for quantifying the complexity of rs-fMRI signals.

Keywords Complexity · Self-resemblance · Fractal · Multi-scale entropy · MSE · Sample entropy · Resting state fMRI · Aging

R. X. Smith (✉) · L. Yan · D. J. J. Wang
Laboratory of Functional MRI Technology (LOFT) Department of Neurology, UCLA, Los Angeles, CA, USA
e-mail: smith.x.robert@gmail.com

D. J. J. Wang
e-mail: jwang71@gmail.com

Introduction

The human brain is one of the most complex information processing systems with 10-100 billion neurons and 10^{14} synapses. Various neurological diseases and disorders are known to affect the ability of the brain to function, in multiple capacities, over multiple time scales. The ability to discern between the severities of these conditions on the capacity of brain function is crucial to understanding their evolution. During the past few decades, a variety of measures derived from the fields of nonlinear statistics and information theory have been developed to describe the dynamics of physiological systems (Goldberger 1996). Many of these are based on the concept of fractals (Mandelbrot 1982). Fractal processes are characterized by "self-resemblance" over multiple measurement scales, and their frequency spectra typically show an inverse power-law (f^{-1}-like) scaling pattern (Goldberger and West 1987; He 2011; Ciuciu et al. 2012).

One of the most widely used non-linear statistics to quantify regularity in serial data of biological systems is approximate entropy (ApEn) introduced by Pincus in 1991 (Pincus 1991). ApEn and its variants such as Sample Entropy (SampEn) (Richman and Moorman 2000) measure the logarithmic likelihood (or conditional probability) that runs of patterns that are close (within the same tolerance width r) for m contiguous observations remain close on subsequent incremental comparisons ($m + 1$). Higher ApEn values generally implicate that the process is less predictable (or more complex). ApEn and SampEn have been successfully applied to biological signals such as cardiac electric activity (ECG), heart rate, blood pressure, respiratory patterns, brain electric activity (EEG), mood ratings, and hormonal release, to distinguish healthy function from disease, and to predict the onset of

adverse health-related events (Abasolo et al. 2005; Kaplan et al. 1991; Pincus 2006; Pincus and Keefe 1992; Ryan et al. 1994; Schuckers and Raphisak 1999). A general trend of decreasing complexity of physiological signals with aging has also been reported (Lipsitz 2004; Pincus 2006).

Resting state fMRI (rs-fMRI) based on the blood-oxygen-level-dependent (BOLD) contrast displays many features indicative of fractal behavior such as a f^{-1} power spectrum (Bullmore et al. 2004; Wang et al. 2003; Zarahn et al. 1997). To date, however, the analysis of resting state BOLD fMRI has been limited to conventional linear statistics such as cross-correlation and amplitude of low frequency fluctuations (Biswal et al. 2010; Yang et al. 2007). Evidence from both task-based fMRI studies and animal electrophysiology suggests that rs-fMRI time series possess non-stationary properties with dynamic changes in functional connectivity within time scales of seconds to minutes (Chang and Glover 2010). In the investigation of non-stationary time series, linear statistical methods such as Fourier analysis performs poorly since it is based on a global, location insensitive frequency representation. Based on these theoretical grounds, we (Liu et al. 2012) and others (Sokunbi et al. 2011), have recently explored the use of ApEn as an index for the complexity and regularity of BOLD fMRI time-series in healthy young and elderly populations as well as in subjects associated with familial Alzheimers disease (fAD). Consistent with existing studies on the complexity of physiological signals, ApEn of BOLD fMRI was found to decrease with normal aging as well as deteriorating cognitive/behavioral performance (Liu et al. 2012; Sokunbi et al. 2011).

One limitation of using ApEn (or SampEn) as an index for the complexity of rs-fMRI, however, is that the entropy may not be directly interpreted as the degree of complexity, since random noise yields the highest entropy but does not represent the most complex process. In addition, experimental confounds such as thermal system noise, physiological noise and limitations on the signal length may inject a considerable amount of uncertainty at the typical time scale or sampling rate of ~0.5 Hz (TR ~ 2 s) in rs-fMRI. Multi-scale entropy (MSE) analysis (Costa et al. 2002) was developed to exploit the fractal scaling behavior in many complex systems by calculating the entropy of a signal at multiple time scales. In MSE analysis, a series of entropy values are calculated on coarse-grained time series that are constructed by averaging the original time series over a range of time scales. Systems with a f^{-1} power spectrum exhibit constant entropy over various time scales (due to their fractal properties), whereas random noise shows a marked decrease in entropy at longer time scales (as random fluctuations are smoothed out). The primary purpose of the present study was to explore MSE analysis to investigate the spatial and temporal characteristics of the entropy of rs-fMRI signals across multiple time scales ($0.05\ Hz < f < 0.5\ Hz$) in healthy subjects. The second purpose of this study was to apply MSE analysis to investigate the healthy aging effect on the complexity of rs-fMRI. We hypothesized that MSE of rs-fMRI in gray matter resembles that of f^{-1} time series, and MSE at longer time scales shows greater age related decline than MSE at the original time scale of 1 (Smith et al. 2013).

Theory

MSE analysis is based on sample entropy (SampEn) which is a variant of ApEn that is robust to the underestimation of entropy when the match count is low (Richman and Moorman 2000):

$$SampEn(m, r, N) = -log\frac{C^{m+1}(r)}{C^{m}(r)}, \tag{1}$$

where m is the pattern length, r is a distance threshold, and N is the length of the time series. C^m(r) is the correlation sum and measures the average likelihood that m-length patterns in data recur as a function of resolution:

$$C^{m}(r) = \frac{1}{(N-m)}\sum_{i,j=0}^{N-m+1}\frac{\Theta\left(r - \parallel u_i^m - u_j^m \parallel\right)}{N-m+1}, \tag{2}$$

where u_i and u_j are two patterns of length m and Θ is the Heavyside function. Two patterns match if the distance is less than a selected threshold value, r. In this study the distance is calculated using the maximum norm, i.e. the maximum absolute component-wise difference. The process is repeated for $m + 1$-length patterns. The ratio between these two values is the average conditional probability that if two m-length patterns match for a given threshold r, then they will continue to match for an additional time point. Figure 1 illustrates the calculation of SampEn on rs-fMRI signals at the original time scale of 1.

MSE analysis investigates the entropy of longer time scale fluctuations by filtering out high frequency fluctuations through a coarse graining procedure of the original signal where τ-consecutive points are averaged to create a new time series of length N/τ.

$$y_i^{\tau} = \frac{1}{\tau}\sum_{i}^{i+\tau-1} x_i \tag{3}$$

where τ is the time scale.

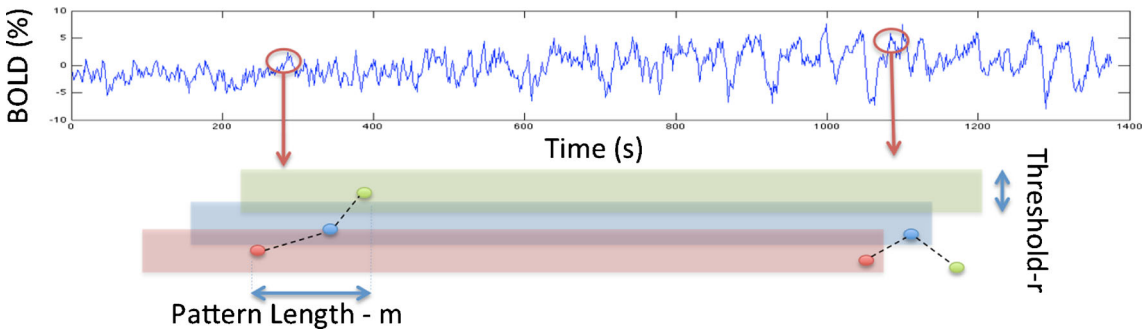

Fig. 1 Illustration of the calculation of SampEn of rs-fMRI at the original time scale of 1 with a pattern length of m and a threshold of r. Here the red-blue patterns will be considered a match for m = 2, but the red-blue-green patterns will not be counted for m = 3, indicating an irregular process

Methods and materials

Subjects

Two experiments (E1, E2) were performed to investigate the spatiotemporal characteristics of MSE analysis of rs-fMRI in healthy young subjects as well as the aging effect on the complexity of rs-fMRI, respectively. Five healthy young subjects (age 21 ± 2 years, 3 female, 2 male) participated in E1, and a total of 16 healthy subjects, 8 young (age 23 ± 2 yrs, 6 males) and 8 elderly subjects (age 66±3 yrs, 5 males), participated in E2. Written informed consents were obtained from all participants who were screened for neurological or psychiatric illnesses.

Data acquisition

All MRI experiments were performed on Siemens TIM Trio 3T scanners (Erlangen, Germany) using 12-channel head coil. In E1 subjects underwent a long resting-state BOLD fMRI scan with their eyes open, using standard gradient-echo echo-planar imaging (EPI). Imaging parameters were - FOV=256 mm; TR=1370 ms; matrix= [64, 64]; 1000 time points; TE = 30 ms (10 ms was also collected for a single volunteer); flip angle=57°; 27 slices with 4 mm thickness. Respiratory and pulse signals were not collected for E1.

In E2 a single-shot dual-echo gradient-echo EPI sequence was used. Each scan with 240 acquisitions took 8 min. Ten oblique slices with 5 mm thickness and 1 mm gap were scanned parallel to the anterior-posterior commissure (AC-PC). Other parameters included - FOV = 22 cm; matrix = [64, 64]; TR = 1000 ms (effective TR = 2000 ms); flip angle= 65° (Liu et al. 2012). Respiratory and pulse signals were recorded in realtime using respiratory belt and pulse-oximetry for E2.

In both E1 and E2 conventional T_1 weighted 3D images were acquired using an MPRAGE sequence (TR / TE / TI = 1730 / 3.96 / 1100 ms; flip angle = 15°; matrix = [256, 256, 192]; voxel size = $1 \times 1 \times 1$ mm^3) for anatomic MRI.

Data processing

The following preprocessing steps were performed for E1: 1) The fMRI data were realigned to correct for motion using FSL's MCFLIRT function (FMRIB, Oxford, UK), 2) the motion effects were further reduced by regression analysis using the 6 rigid-body motion parameters of translation displacements and rotation angles across rs-fMRI time series, 3) linear trends were then regressed out. The same process was performed for E2 but cardiac and respiratory signals were collected and corrected for using RETROICOR. No other regressors (e.g. white matter/CSF, or global signal) were used.

Whole brain MSE analysis is performed voxelwise using a custom MATLAB program. A threshold size of $r = 0.3$ is used in this report. To gain an understanding of the effect of the threshold parameter, we perform the MSE analysis for an additional threshold size $r = 1.3$. However, with the exception of reduced SampEn values, no significant changes to the results presented in this report were found. Due to increasing pattern overlap decreasing SampEn's statistical power, previous reports have indicated the parameter length, m, should be set such that m∼log(N), where N is the length of the time series. A pattern length of $m = 2$ is used for both E1 ($N = 1000$), and E2 ($N = 220$). The mean volume of the motion corrected time series was co-registered to the T1-weighted structural MRI. Whole-brain gray matter, white matter, and cerebrospinal fluid (CSF) masks were segmented based on T1-weighted structural MRI. Average MSE values of gray matter, white matter, and CSF were calculated using the corresponding masks in each subject.

Statistical analyses

Group statistics are performed with a multivariate t-test using Hotelling's T^2-distribution. Entropy values at different scales become components of an 'entropy vector'. Group statistics are based on comparing the distance between mean entropy vectors normalized by a pooled covariance matrix, and adjusted for multiple comparisons within the gray matter volume. This method is preferable to separate univariate t-tests conducted at each scale, as all data exhibit some level of positive correlation due to the presence of noise. To test the null hypothesis that the entropy values are dominated by random fluctuations, MSE analysis (using the same $m = 2$ and $r = 0.3$, 1.3 values) was performed on ten thousand white noise time series of equal length to the voxel time series. The same process was undergone to test for the null hypothesis that the entropy values arise from f^{-1} ('pink') noise time series. Pink noise time series were generated by applying a f^{-1} frequency filter to a generated white noise frequency spectrum followed by an inverse fast Fourier transform.

Results

Spatiotemporal characteristics of MSE analysis of rs-fMRI (E1)

Figure 2 shows the effect of motion on the group mean gray and white matter entropy values for E1 (N = 1000) subjects over multiple time scales. The increase SampEn after motion correction for both gray and white matter point to the presence of rhythmic motion, e.g. respiratory motion. For comparison, entropy for Gaussian distributed uncorrelated (white) noise and correlated (pink - f^{-1}) noise at multiple time scales are shown. At shorter time scales motion corrected gray matter exhibits entropy values falling in between f^{-1} and white noise, whereas motion corrected white matter shows very similar values to white noise. However, at longer time scales (lower temporal frequencies) motion corrected gray matter exhibits higher entropy values compared to white matter. Overall, MSE of gray matter, rather than white matter, closely resembles that of f^{-1} noise. We further tested for the effect of physiological noise on the average gray matter entropy of the young subject data sets (E2) by regressing out cardiac and respiratory fluctuations using RETROICOR (Glover et al. 2000), however, the effect is very weak.

To test if the entropy difference between gray and white matter is due at least in part to the presence of spontaneous fluctuations in the gray matter, a TE = 10 ms, 4D data set is collected and compared to a TE = 30 ms, 4D data set (both with 1000 time points). Figure 3 shows that increasing TE from 10 ms to 30 ms, a greater than 10 % increase in the average gray matter entropy is seen at the highest scale, while a smaller than 5 % increase is seen in the average white matter entropy. This indicates that SampEn is sensitive to the presence of spontaneous fluctuations and changes thereof.

Figure 4 shows the group mean entropy images of three slices at four different scales ($\tau = 1$, 4, 7, and 10). The shortest time scale, $\tau = 1$, corresponds to the original signal. At the shortest scale the entropy is dominated by the high frequency fluctuations from random noise. By filtering these fluctuations out the contrast in entropy becomes much sharper between gray and white matter at longer time scales.

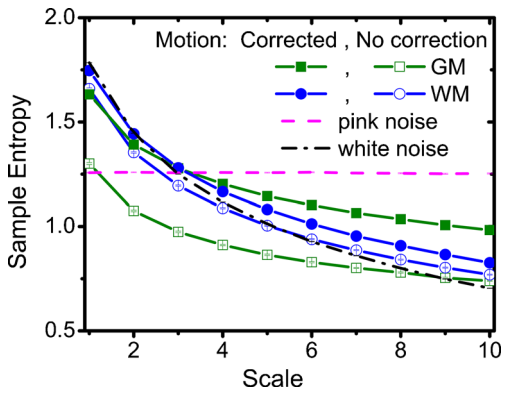

Fig. 2 Group average gray matter and white matter SampEn over multiple time scales, before and after motion correction. SampEn of Gaussian-distributed uncorrelated (*white*) and correlated (pink f^{-1}) noise are plotted for comparison

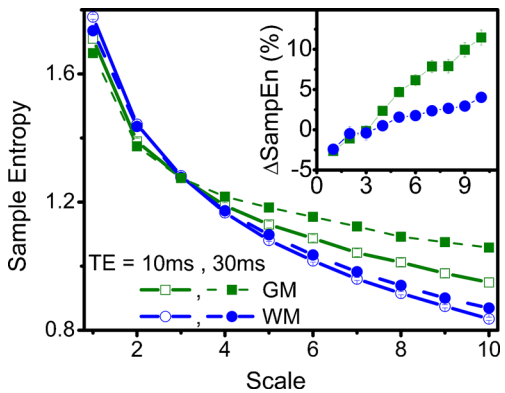

Fig. 3 Test for the effect of spontaneous fluctuations on entropy. Comparison of average SampEn for gray matter and white matter for a single volunteer over multiple time scales at TE=10 ms and TE=30 ms. The latter is the approximate time for optimal BOLD contrast. The inset shows the percent change in entropy as TE is increased from 10 ms to 30 ms. The displayed error bars are approximately the size of the symbols

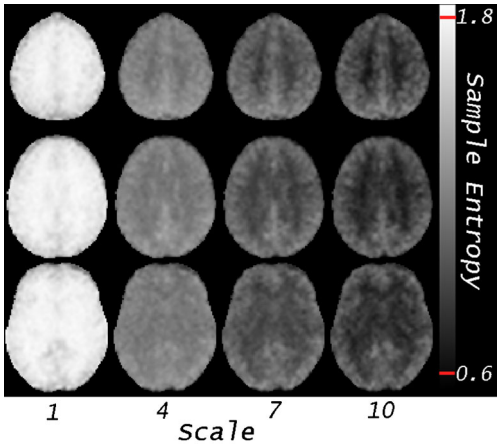

Fig. 4 Group mean SampEn images for three slices, Z = 36, 48, and 59 (*bottom, middle, and top*, respectively) in MNI space, of five volunteers at scales 1, 4, 7, and 10

Aging effects on MSE of rs-fMRI (E2)

Figure 5 shows average gray matter entropy values for 8 young volunteers (age 23±2 yrs) and 8 aged volunteers (age 66 ± 3 yrs). Each group exhibits a similar drop in entropy with increasing scale. Entropy values at low scales are similar between the two groups on account of the dominance of noise at short time scales. By filtering out random fluctuations in rs-fMRI, the entropy difference between the young and elderly subjects became more apparent at longer time scales. Figure 6 shows significant differences between the two age groups ($p < 0.05$, with Bonferroni correction) in the following regions: thalamus, caudate, lingual gyrus, hippocampus, supramarginal gyrus, superior temporal cortex, and areas associated with the default mode network (middle temporal gyrus, anterior cingulate cortex, left and right angular cortex, middle and superior frontal cortex).

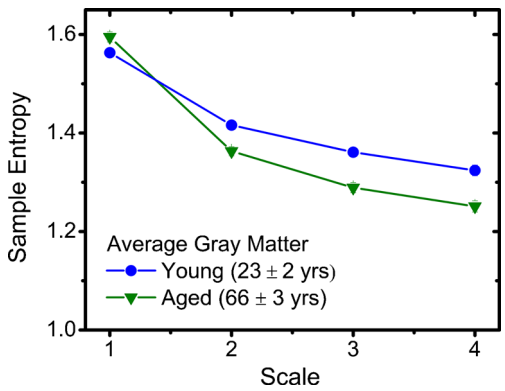

Fig. 5 Average gray matter entropy for 8 young volunteers (age 23±2 years) and 8 aged volunteers (age 66 ± 3 years). Plotted error bars are four standard errors of the respective means, p < 10^{-4}, and approximately the size of the symbols

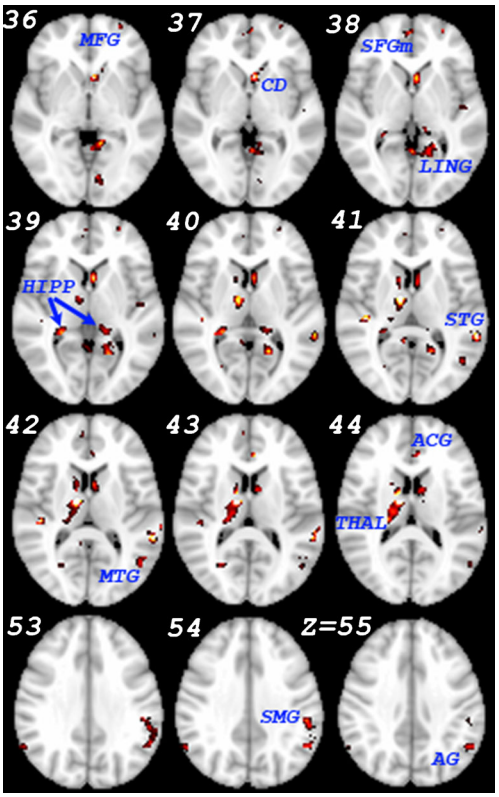

Fig. 6 Increased regional MSE in young subjects. Images show results of multivariate two sample *t* test comparing healthy young subjects versus healthy aged subjects. Only clusters with 18 or more activated voxels ($p < 0.05$, corrected) are shown. Decreases in MSE in older subjects are seen in regions associated with the default mode network: middle temporal gyrus - MTG, anterior cingulate gyrus - ACG, left and right angular gyrus - AG, middle and superior medial frontal cortex - MFG, SFGm. Significant decreases are also seen in the thalamus - THAL, caudate - CD, the lingual gyrus - LING, the hippocampus -HIPP, the supramarginal gyrus - SMG, and the superior temporal gyrus - STG. The numbers to the top left of each image refer to the z coordinate in MNI space

Discussion

In the present study, we explored MSE analysis of rs-fMRI using a long scan with 1000 data points in healthy young subjects. White and gray matter both exhibit drops in entropy with increasing scale similar to the behavior of white noise. However, the average entropy in gray matter exhibits slightly smaller values at the shortest timescale but experience a significantly smaller drop than the average white matter values with increasing scale. This increased entropy in gray matter at higher scales resides closer to that of f^{-1} noise, compared to entropy values in white matter. By filtering out high frequency random fluctuations, the entropy contrast between gray and white matter became apparent with the former greater than the latter at longer time scales. In our pilot study on ApEn analysis of rs-fMRI (i.e., MSE at the original time scale of 1), white matter

showed significantly higher ApEn values than gray matter, which has been attributed to a greater fraction of white noise in white matter than in gray matter (Liu et al. 2012). Due to sample entropy's sensitivity to white noise, the observed difference between gray and white matter entropy is partly reflective of the relative differences in SNR. However, MSE analysis reduces this sensitivity by averaging out short time scale fluctuations. While the MSE of white matter exhibits values closer to white noise than gray matter, it is still statistically dissimilar to white noise at longer time scales, indicating the presence of additional fluctuations.

It has been demonstrated by Logothetis et al. (2001) that hemodynamic responses in the BOLD signal correlate best with local field potentials (LFT) that are thought to reflect the weighted average of input signals on the dendrites and cell bodies of local neurons. Therefore a higher level of complexity or entropy value of rs-fMRI is expected in gray matter than white matter, given the distribution of dendrites and cell bodies of neurons in gray matter. We sought to determine if the white matter - gray matter difference in entropy arises from the presence of spontaneous fluctuations. We compare the average entropies for a single subject collected at two echo times, 10 ms and 30 ms. The latter TE manifests greater BOLD effects than the former TE. At long time scales the average entropy at TE $=$ 30 ms exhibits larger values over those calculated for TE $=$ 10 ms, while the reverse holds true at small time scales. We further investigated the effect of motion and physiological noise on the average gray and white matter entropy. An increase in entropy is seen for all scales for both gray and white matter, possibly arising from a decrease in rhythmic behavior, with gray matter exhibiting approximately double the increase of white matter due. Our data suggest that MSE analysis is effective in smoothing out high frequency random fluctuations and thereby revealing the inherent complexity of spontaneous neuronal activities in rs-fMRI.

At longer time scales, MSE analysis showed greater age related decline in the average gray-matter complexity of resting state BOLD fMRI compared to the original time scale of 1 (Fig. 5). Using a multivariate t test, increased activity in younger versus older subjects ($p < 0.05$, corrected) is seen in the default mode network containing the middle temporal cortex, the superior and middle frontal cortex, anterior cingulate cortex, and bilateral activation in the angular cortex. This is consistent with previous reports (Damoiseaux et al. 2008), using an ICA based approach to measure activity. Additionally, the MSE analysis results presented here show decreased activation in the older subjects in the hippocampus, an area involved with episodic memory processing, consistent with ICA and event-related results (Greicius et al. 2004; Daselaar et al. 2006). Large regions of decreased MSE activation in the older group are seen in the thalamus and caudate, areas involved in learning and memory. Interestingly, a recent report has shown decreased diffusion and increased fractional anisotropy in the basal ganglia with age (Wang et al. 2010). Our results are consistent with a recent study that explored MSE analysis on rs-fMRI data of 99 healthy elderly and 56 younger subjects (Yang et al. 2013). MSE of BOLD signals from default mode network (DMN) areas were found to be positively correlated with cognitive functions and negatively correlated with aging. It has been suggested that normal human aging is associated with a loss of complexity in a variety of fractal-like anatomic structures and physiological processes (Lipsitz 2004; Pincus 2006). Techniques employing fractal-based analyses have shown aging to be associated with a loss of complexity in blood pressure, respiratory cycle, stride interval, and postural sway dynamics (Goldberger et al. 2002; Kaplan et al. 1991; Peng et al. 2002). Further, aging may degrade cortical and sub-cortical connections through cell loss, synaptic degeneration, blood flow reduction, neurochemical alteration as well as central nervous system reorganization (Craik and Salthouse 2000). Taken together, age-related changes may facilitate the erosion of both local and long-range connections in the brain, decreasing the complexity of spontaneous brain activity. The age related decline in MSE of rs-fMRI at longer time scales, observed in the present study, is therefore consistent with past findings. This result also supports the validity of MSE analysis for detecting aging effects on the complexity of rs-fMRI in the presence of confounding random noise.

One limitation of the MSE analysis is that the length of each coarse-grained time series is equal to the length of the original time series divided by the scale factor. Therefore, coarse-grained procedures in MSE with large scale factors may result in short data length and subsequently unreliable entropy estimation. As suggested by prior studies, the estimation of ApEn requires signal lengths of 10^m to 20^m (m: pattern length) (Richman and Moorman 2000). Multiband EPI is a recent technical advance of fMRI by performing parallel imaging in the form of multiband radiofrequency excitation, in conjunction with k-space under-sampling in the phase-encode direction (Feinberg et al. 2010; Moeller et al. 2010). Up to 16-fold acceleration ($\times 4$ multiband, $\times 4$ phase under-sampling) can be achieved allowing whole brain fMRI with high spatial (a few mm^3) and/or temporal resolutions (TR $\leq$ 1 s). It is expected that multiband EPI will accelerate rs-fMRI and increase the signal length by at least 4-fold (TR $\sim$ 500 ms) compared to standard EPI (TR $= 2 \sim 3$ s), allowing more reliable MSE analysis. This is an important direction to pursue in further development of MSE analysis of rs-fMRI.

Conclusion

Multi-scale entropy analysis is a promising nonlinear statistical approach for assessing the complexity of rs-fMRI signals across multiple time scales. By filtering out high frequency random fluctuations, MSE analysis was able to reveal enhanced contrast in entropy between gray and white matter, as well as between age groups.

Acknowledgments This study was supported by US National Institutes of Health grants R01-MH080892, R01-NS081077, R01-EB014922 and California Department of Public Health Grant Agreement No. 13-12008. The software used in this paper can be downloaded at: http://www.fil.ion.ucl.ac.uk/spm/ext/#Complexity

Disclosure statement

The authors have no conflicts of interest to disclose.

References

Abasolo, D., Hornero, R., Espino, P., Poza, J., Sanchez, C., de la Rosa, R. (2005). Analysis of regularity in the eeg background activity of alzheimer's disease patients with approximate entropy. *Clinical Neurophysiology*, *116*, 1826–1834.

Biswal, B., Mennes, M., Zuo, X., Gohel, S., Kelly, C., Smith, S. (2010). Toward discovery science of human brain function. *Proceedings of the National Academy of Sciences of the United States of America*, *107*, 4734–4739.

Bullmore, E., Fadili, J., Maxim, V., Sendur, L., Whitcher, B., Suckling, J., et al. (2004). Wavelets and functional magnetic resonance imaging of the human brain. *NeuroImage*, *23*.

Chang, C., & Glover, G. (2010). Time-frequency dynamics of resting-state brain connectivity measured with fmri. *NeuroImage*, *50*, 81–98.

Ciuciu, P., Varoquaux, G., Abry, P., Sadaghiani, S., Kleinschmidt, A. (2012). Scale-free and multifractal properties of fmri signals during rest and task. *Frontiers in Physiology*, *3*(186).

Costa, M., Goldberger, A., Peng, C. (2002). Multiscale entropy analysis of complex physiologic time series. *Physical Review Letters*, *89*.

Craik, F., & Salthouse, T. (2000). The handbook of aging and cognition. Evanston: Routledge.

Damoiseaux, J.S., Beckmann, C.F., Arigita, E.J.S., Barkhof, F., Scheltens, P., Stam, C.J., et al. (2008). Reduced resting-state brain activity in the "default network" in normal aging. *Cerebral Cortex*, *18*(8), 1856–1864.

Daselaar, S.M., Fleck, M.S., Dobbins, I.G., Madden, D.J., Cabeza, R. (2006). Effects of healthy aging on hippocampal and rhinal memory functions: an event-related fmri study. *Cerebral Cortex*, *16*(12), 1771–1782.

Feinberg, D., Moeller, S., Smith, S., Auerbach, E., Ramanna, S., Gunther, M., et al. (2010). Multiplexed echo planar imaging for sub-second whole brain fmri and fast diffusion imaging. *PLoS One*, *5*.

Glover, G., Li, T.-Q., Ress, D. (2000). Image-based method for retrospective correction of image-based method for retrospective correction of physiological motion effects in fmri: Retroicor. *MRM*, *44*.

Goldberger, A. (1996). Non-linear dynamics for clinicians: chaos theory, fractals, and complexity at the bedside. *Lancet*, *347*, 1312–1314.

Goldberger, A., & West, B. (1987). Fractals in physiology and medicine. *The Yale Journal of Biology and Medicine*, *60*, 421–435.

Goldberger, A., Amaral, L., Hausdorff, J., Ivanov, P., Peng, C., Stanley, H. (2002). Fractal dynamics in physiology: alterations with disease and aging. *Proceedings of the National Academy of Sciences of the United States of America*, *99*, 2466–2472.

Greicius, M.D., Srivastava, G., Reiss, A.L., Menon, V. (2004). Default-mode network activity distinguishes alzheimer's disease from healthy aging: evidence from functional mri. *Proceedings of the National Academy of Sciences of the United States of America*, *101*(13), 4637–4642.

He, B.J. (2011). Scale-free properties of the functional magnetic resonance imaging signal during rest and task. *The Journal of Neuroscience*, *31*(39), 13786–13795.

Kaplan, D., Furman, M., Pincus, S., Ryan, S., Lipsitz, L., Goldberger, A. (1991). Aging and the complexity of cardiovascular dynamics. *Biophysical Journal*, *59*, 945–949.

Lipsitz, L. (2004). Physiological complexity, aging, and the path to frailty. *Science of Aging Knowledge Environment*, *16*.

Liu, C., Krishnan, A., Yan, L., Smith, R., Kilroy, E., Alger, J., et al. (2012). Complexity and synchronicity of resting state blood oxygenation level-dependent (BOLD) functional MRI in normal aging and cognitive decline. *Journal of Magnetic Resonance Imaging*, *38*, 36–45.

Logothetis, N.K., Pauls, J., Augath, M., Trinath, T., Oeltermann, A. (2001). Neurophysiological investigation of the basis of the fmri signal. *Nature*, *412*, 150–157.

Mandelbrot, B. (1982). The fractal geometry of nature. San Francisco: Freeman.

Moeller, S., Yacoub, E., Olman, C., Auerbach, E., Strupp, J., Harel, N., et al. (2010). Multiband multislice ge-epi at 7 tesla, with 16-fold acceleration using partial parallel imaging with application to high spatial and temporal whole-brain fmri. *Magnetic Resonance in Medicine*, *63*, 1144–1153.

Peng, C., Mietus, J., Liu, Y., Lee, C., Hausdorff, J., Stanley, H., et al. (2002). Quantifying fractal dynamics of human respiration: age and gender effects. *Annals of Biomedical Engineering*, *30*, 683–692.

Pincus, S. (1991). Approximate entropy as a measure of system complexity. *Proceedings of the National Academy of Sciences of the United States of America*, *88*, 2297–2301.

Pincus, S. (2006). Approximate entropy as a measure of irregularity for psychiatric serial metrics. *Bipolar Disorders*, *8*, 430–440.

Pincus, S., & Keefe, D. (1992). Quantification of hormone pulsatility via an approximate entropy algorithm. *The American Journal of Physiology*, *262*, E741–E754.

Richman, J., & Moorman, J. (2000). Physiological time-series analysis using approximate entropy and sample entropy. *American Journal of Physiology, Heart and Circulatory Physiology*, *278*, H2039–H2049.

Ryan, S., Goldberger, A., Pincus, S., Mietus, J., Lipsitz, L. (1994). Gender- and age-related differences in heart rate dynamics: are women more complex than men? *Journal of the American College of Cardiology*, *24*, 1700–1707.

Schuckers, S., & Raphisak, P. (1999). Distinction of arrhythmias with the use of approximate entropy. *Computers in Cardiology*, *26*, 347–350.

Smith, R., Yan, L., Wang, D. (2013). Multiple time scale entropy of resting state fMRI. In *Proceedings of the international society of magnetic resonance in medicine, Oral Presentation*.

Sokunbi, M., Staff, R., Waiter, G., Ahearn, T., Fox, H., Deary, I., et al. (2011). Inter-individual differences in fMRI entropy measurements in old ag. *IEEE Transactions on Bio-medical Engineering*, *58*, 3206–3214.

Wang, J., Aguirre, G., Kimberg, D., Roc, A., Li, L., Detre, J. (2003). Arterial spin labeling perfusion fMRI with very low task frequency. *Magnetic Resonance in Medicine*, *49*, 796–802.

Wang, Q., Xu, X., Zhang, M. (2010). Normal aging in the basal ganglia evaluated by eigenvalues of diffusion tensor imaging. *American Journal of Neuroradiology*, *31*(3), 516–520.

Yang, H., Long, X., Yang, Y., Yan, H., Zhu, C., Zhou, X. (2007). Amplitude of low frequency fluctuation within visual areas revealed by resting-state functional MRI. *NeuroImage*, *36*, 144–152.

Yang, A., Huang, C., Yeh, H., Liu, M., Hong, C., Tu, P., et al. (2013). Complexity of spontaneous BOLD activity in default mode network is correlated with cognitive function in normal male elderly: a multiscale entropy analysis. *Neurobiology of Aging*, *34*, 428–438.

Zarahn, E., Aguirre, G., D'Esposito, M. (1997). Empirical analyses of BOLD fMRI statistics. I. Spatially unsmoothed data collected under null-hypothesis conditions. *NeuroImage*, *5*, 179–197.